

SA-CME Information

A Multimodality Approach to Imaging the Mediastinum and Pleura: Pearls and Pitfalls

Description

Diagnostic interpretation of cross-sectional imaging of the mediastinum and pleura presents unique and significant challenges even to the experienced radiologist. The mediastinum is anatomically complex, comprising numerous structures arranged into multiple anatomic compartments that can give rise to a wide range of pathologies. The pleural space is thin and multi-planar, which can confound evaluation and quantification of pleural abnormalities.

In this article, we will review imaging approaches to the mediastinum and pleura and present imaging pearls and pitfalls that can assist radiologic interpretation. This will include common masses that present in routine imaging of the chest and key imaging features that help to distinguish them using CT, MRI and FDG-PET/CT.

The knowledge of common mediastinal and pleural pathologies present on cross-sectional imaging will enable the radiologist to make informed diagnostic radiologic interpretations and guide appropriate intervention and surveillance.

Learning Objectives

After completing this activity, the participant will be able to:

- Explain the basic anatomy of the mediastinum and pleura and common pitfalls in diagnostic interpretation of masses in these anatomical spaces.
- Describe the strengths and weaknesses of CT, MRI, and FDG-PET/CT in problem-solving indeterminate masses in the mediastinum and pleura.
- Distinguish the features of common masses in the mediastinum and pleura in order to generate an accurate differential diagnosis.

Accreditation/Designation Statement

The Institute for Advanced Medical Education is accredited by the Accreditation Council for Continuing Medical Education (ACCME) to provide continuing medical education for physicians.

The Institute for Advanced Medical Education designates this journal-based CME activity for a maximum of *1 AMA PRA Category 1 Credit™*. Physicians should only claim credit commensurate with the extent of their participation in the activity.

These credits qualify as SA-CME credits.

Authors

Leonid Roshkovan, MD, and Sharyn Katz, MD, MTR, are Professors of Radiology at the University of Pennsylvania Perelman School of Medicine, and Radiologists at the Hospital of the University of Pennsylvania, Philadelphia, PA. The authors declare no conflicts of interest. Some of the material in this manuscript was presented at the Penn 41st Diagnostic Imaging on the Cape CME course.

Target Audience

- Radiologists
- Related Imaging Professionals

System Requirements

In order to complete this program, you must have a computer with a recently updated browser and a printer. For assistance accessing this course online or printing a certificate, email CustomerService@AppliedRadiology.org.

Instructions

This activity is designed to be completed within the designated time period. To successfully earn credit, participants must complete the activity during the valid credit period. To receive SA-CME credit, you must:

1. Review this article in its entirety.
2. Visit www.appliedradiology.org/SAM2.
3. Login to your account or (new users) create an account.
4. Complete the posttest and review the discussion and references.
5. Complete the evaluation.
6. Print your certificate.

Estimated time for completion: **1 hour**

Date of release and review: **March 1, 2020**

Expiration date: **February 28, 2022**

Disclosures

No authors, faculty, or any individuals at IAME or *Applied Radiology* who had control over the content of this program have any relationships with commercial supporters.

A Multimodality Approach to Imaging the Mediastinum and Pleura: Pearls and Pitfalls

Leonid Roshkovan, MD; Sharyn I. Katz, MD, MTR

Diagnostic interpretation of cross-sectional imaging of the mediastinum and pleura presents unique and significant challenges even to the experienced radiologist. The mediastinum is anatomically complex, comprising numerous structures arranged into multiple anatomic compartments that can give rise to a wide range of pathologies. The pleural space, moreover, is thin and multiplanar, which can confound evaluation and quantification of pleural abnormalities.

Here we review imaging approaches to the mediastinum and pleura and present imaging pearls and pitfalls that can assist radiologic interpretation. This will include common masses that present in routine imaging of the chest, as well as the key imaging features that help to distinguish them using computed tomography (CT), magnetic resonance imaging (MRI) and 18F-fluorodeoxyglucose positron-emission tomography/computed tomography (FDG-PET/CT).

The knowledge of common mediastinal and pleural pathologies present on cross-sectional imaging will enable

the radiologist to make informed diagnostic radiologic interpretations and guide appropriate intervention and surveillance.

Anatomy of the Mediastinum

The standard radiologic classification of mediastinal anatomy is based on the three-compartment model (anterior, middle, and posterior) based on landmarks on the lateral chest X-ray.^{1,2} With the thoracic inlet forming the superior border and the diaphragm representing the inferior border in this system, the anterior compartment includes structures anterior to the pericardium. The middle compartment includes structures between the heart and spine. The posterior compartment includes structures in the paraspinous location. This is the system most widely used.

More recently, the Japanese Association for Research of the Thymus (JART) introduced a new classification scheme based on CT imaging,³ which was later revised by the International Thymic Malignancy Interest Group (ITMIG).^{4,5} In this system, the mediastinum is also considered to have three compartments, with the thoracic inlet forming the superior border and the diaphragm representing the inferior border.⁴ These compartments are known as the perivascular, visceral, and paravertebral compartments; this system is considered a more accurate approach

to anatomic characterization in the age of cross-sectional imaging.

Imaging the Mediastinum *Chest Radiography*

Chest radiography remains the most common initial test for detecting mediastinal pathology. A differential diagnosis of mediastinal pathology takes into consideration the involved mediastinal compartment and the speed of development, together with factors such as patient age, gender, and comorbidities. Several well-established radiologic signs are used for lesion localization; these include loss of mediastinal interfaces and the silhouette sign.^{1,2} The sensitivity of chest X-rays in identifying small mediastinal lesions, however, is low, particularly for lesions in the posterior mediastinum (6% sensitivity), compared to the paratracheal location (69% sensitivity).⁶ Sensitivity can be improved by obtaining frontal and lateral view chest radiographs.

CT

CT imaging is the modality of choice with respect to characterizing mediastinal pathology.⁷ The superior resolution of modern CT imaging permits accurate localization and provides information on tissue texture and aggressiveness. Measuring tissue attenuation on CT can help differentiate fat (fluid 0-20 HU, soft tissue 20-40 HU and hemorrhage 40-60 HU),⁸ which

Affiliations: University of Pennsylvania Perelman School of Medicine, Philadelphia, PA.

Some of the material in this manuscript was presented at the Penn 41st Diagnostic Imaging on the Cape CME course. The figures are original to this manuscript.

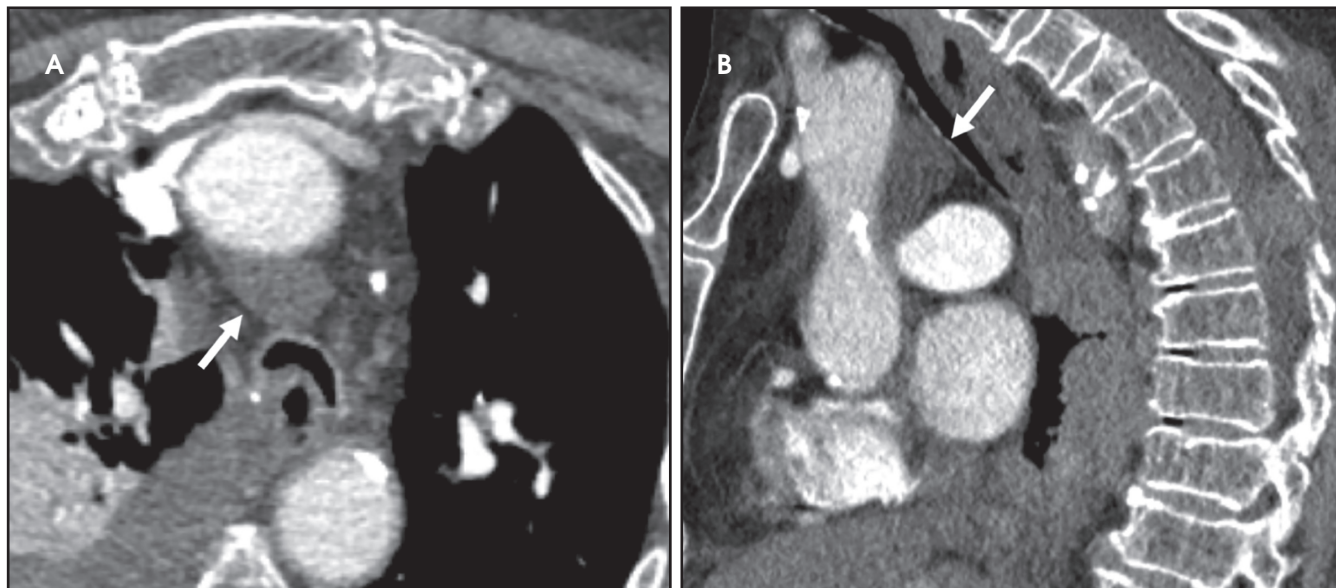


FIGURE 1. Prominent superior pericardial recess. (A) Axial CT of the chest with IV contrast in an 88-year-old with non-small cell lung cancer reveals a focus of fluid attenuation (arrow) projecting in continuity with the posterior surface of the ascending aorta. (B) A sagittal view confirms that this fluid (arrow) tracks along the surface of the aorta and lies within the superior pericardial recess.

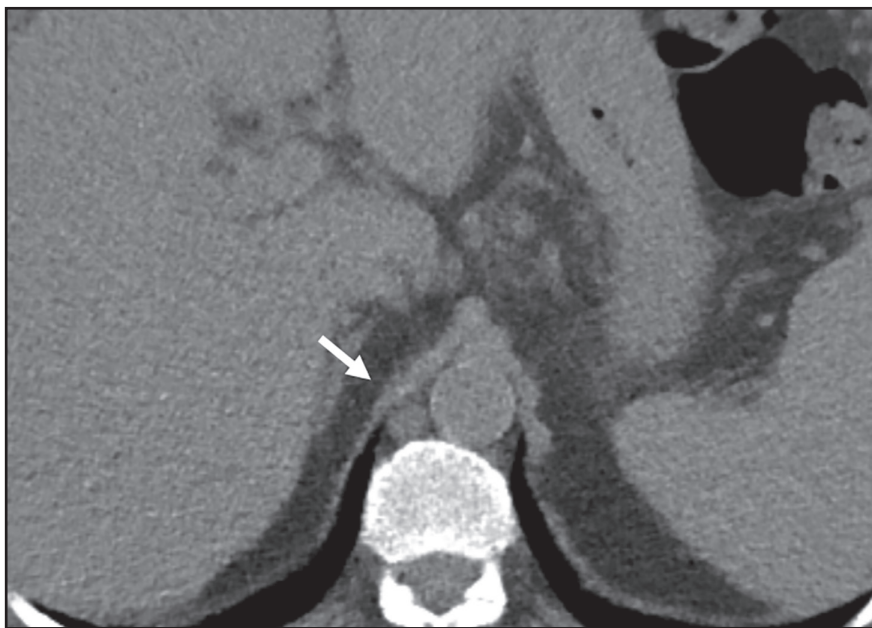


FIGURE 2. Prominent cisterna chylii. Axial unenhanced CT of the chest reveals a prominent fluid attenuation structure (arrow) to the left of the aorta just above the diaphragmatic hiatus in a 65-year-old with hepatocellular carcinoma undergoing surveillance imaging.

CT attenuation. On CT, soft tissue typically demonstrates intermediate signal intensity relative to smooth muscle on T1 and T2 imaging, and proteinaceous fluid demonstrates high signal intensity relative to smooth muscle on T1 and T2 sequences.⁹ MRI can also be used to characterize iron-enriched tissues, such as blood products; to detect the presence of microscopic fat, such as in the setting of thymic hyperplasia;¹⁰ and to characterize the internal complexity of cystic masses, which are not always visible on CT. Diffusion-weighted imaging (DWI) MRI has shown value in distinguishing neoplastic from non-neoplastic lesions considered indeterminate on CT.¹¹

FDG-PET/CT

In addition to detecting occult malignancy in the setting of cancer staging, FDG-PET/CT can be employed to further characterize a mediastinal lesion suspicious for malignancy on CT or MRI. An indeterminate lesion found to be FDG-avid on PET/CT may prompt a biopsy or, in the setting of known primary malignancy, empiric therapy. Conversely, an equivocal lesion on CT found to be FDG-nonavid on PET/CT may be managed conservatively. FDG-PET/CT, however, does suffer

is most accurately measured without intravenous (IV) contrast. Intravenous enhancement often provides additional information on vascularity, textural heterogeneity, and improved definition of lesion boundaries. In many cases, CT provides sufficient information regarding whether and how to intervene therapeutically.

MRI

MRI tissue contrast is superior to that of CT and is sometimes used to refine differential diagnoses, particularly where a benign diagnosis can be confidently established to avoid invasive biopsy. MRI can be used to differentiate between solid tissue and proteinaceous fluid, both of which can demonstrate similar

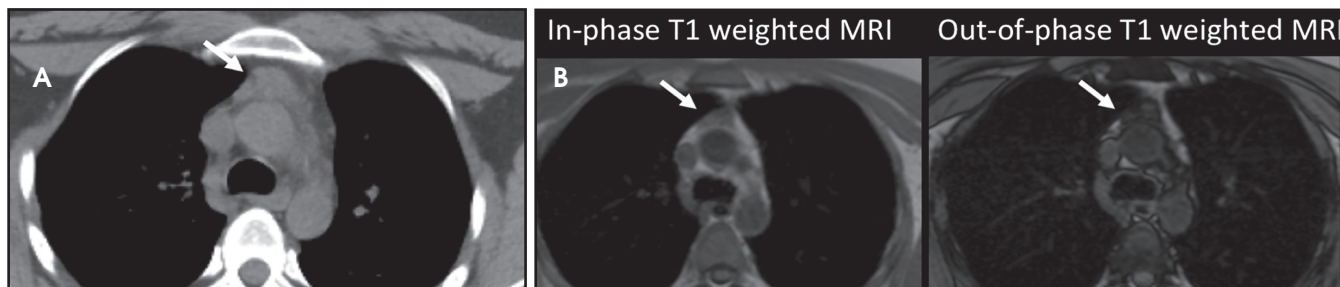


FIGURE 3. Thymic hyperplasia. (A) Axial unenhanced CT of the chest in a 32-year-old with a history of Hodgkin lymphoma reveals soft tissue (arrow) in the anterior mediastinum in the region of the thymus. (B) A uniform drop in tissue signal is observed from in- to out-of-phase T1 imaging within the lesion (arrow), indicating the presence of microscopic fat in keeping with benign thymic hyperplasia.

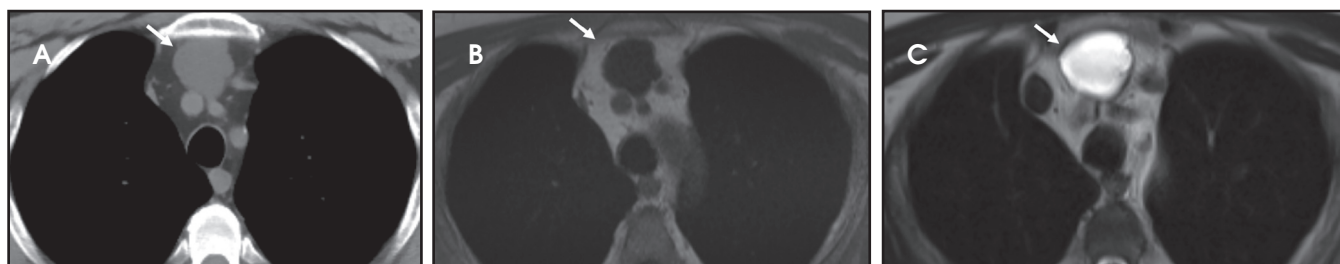


FIGURE 4. Thymic cyst. (A) Axial unenhanced CT of the chest in a 74-year-old with prostate cancer reveals a well-circumscribed, fluid attenuation cystic structure (arrow) in the anterior mediastinum. Further characterization with MRI reveals a uniformly low T1 signal (B) and high T2 signal (C) through the lesion (arrows) without internal solid components, in keeping with a thymic cyst.

from some limitations in sensitivity and specificity for neoplasm. These include lower accuracy for small lesions (<6-8 mm) in the setting of poorly avid or inconsistently avid malignancies, such as some mucin-producing, non-small cell lung cancer,¹² low-grade lymphoma,¹³ and some thyroid malignancies, as well as in the setting of FDG-avid, nonmalignant disease, such as sarcoidosis.¹⁴ As a result, the overall sensitivity and specificity of FDG-PET/CT for distinguishing malignant from benign mediastinal tissue has been reported at 83% and 58%, respectively,¹⁵ although it may be more sensitive and specific in certain clinical settings, such as most non-Hodgkin lymphoma.¹⁶ In addition to detecting malignancy, avidity on FDG-PET/CT can indicate aggressive histology. For example, the degree of FDG avidity can be used to distinguish between high- and low-risk thymomas as well as between thymoma and thymic carcinoma.¹⁷

Multimodality Imaging Applications in the Mediastinum

Pseudolesions of the Mediastinum

Several normal anatomic structures and anatomic variants can mimic disease

in different imaging modalities. The following are a few commonly encountered pitfalls in radiologic interpretation in the mediastinum:

Pericardial Recesses. The pericardium envelopes not only the heart, but also the pulmonary arteries, pulmonary veins, ascending aorta, and superior vena cava. Fluid can collect in the pericardial recesses and be mistaken for lymphadenopathy (Figure 1). The correct diagnosis can be made by carefully analyzing the relationship of the finding to adjacent vascular structures and characteristics of fluid on CT or MRI.¹⁸

Cysterna Chylli. The cysterna chylli is a sac-like dilatation of the lymphatic trunks as they converge to form the origin of the thoracic duct and can be visible in the right lateral para-aortic, retrocrural space. When prominent, the cysterna chylli can be mistaken for retrocrural lymphadenopathy (Figure 2). Clues to the correct diagnosis include familiarity with the location of this structure and characteristics of fluid attenuation on CT or MRI.^{19,20}

Pseudothrombus. Left atrial appendage thrombus is a well-documented complication in patients with

atrial fibrillation; however, it can be mimicked by stasis and poor mixing of blood and contrast material on CT, leading to misdiagnosis. Using delayed phase on either CT or MRI can avoid this pitfall by allowing more time for appropriate mixing of IV contrast in the atrial appendage.^{21,22}

Mediastinal Lipomatosis. This exaggerated deposition of fat in the mediastinum, often related to obesity and steroid treatment, can mimic mediastinal pathology on chest radiography; but it can easily be characterized as amorphous nonencapsulated fat on CT. Imaging with absent internal solid components or evidence of mass effect on adjacent structures,²³ distinguishing it from the malignant, fat-containing neoplasm, liposarcoma.

Differentiating Benign and Malignant Masses

Thymic Hyperplasia

Over the course of a lifetime, the thymus progressively becomes involuted and fatty, with little solid thymic tissue remaining by age 50. However, in certain clinical settings, benign thymic hyperplasia can be mistaken for neoplasm.

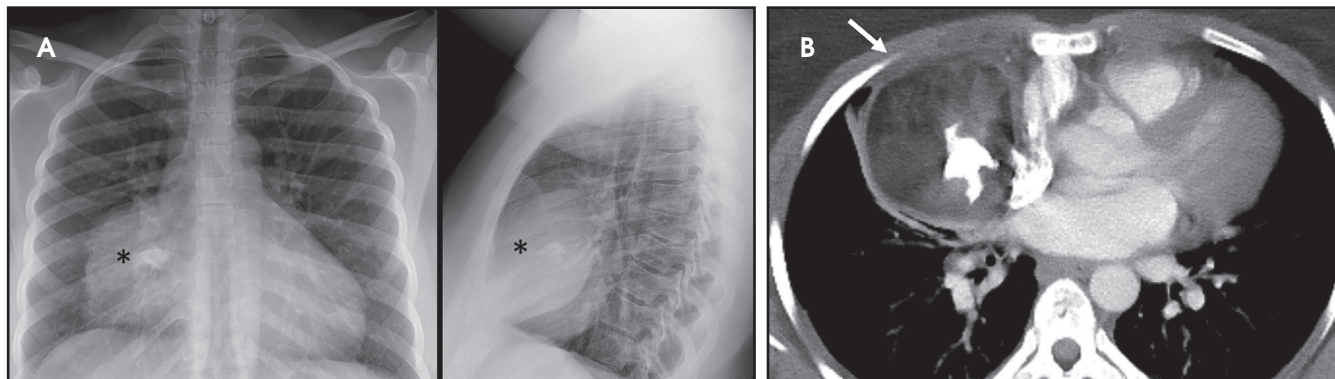


FIGURE 5. Germ cell tumor. (A) PA and lateral chest radiographs reveal an anterior mediastinal mass (*) extending into the right paracardiac space in a 31-year-old. (B) Axial intravenous enhanced CT reveals a well circumscribed mass (arrow) largely composed of macroscopic fat with internal foci of soft tissue attenuation and large coarse calcifications. These features and the young age of the patient suggest the diagnosis of mature cystic teratoma, which was confirmed at surgery.

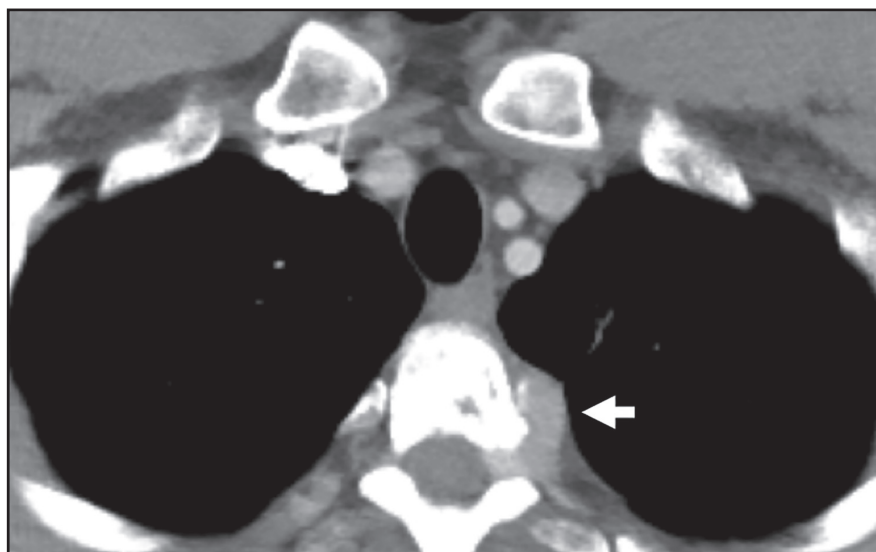


FIGURE 6. Paraspinal paraganglioma. Axial IV contrast-enhanced CT images of the chest in a 38-year-old reveals an elongated enhancing soft tissue insinuating in the T1-2 left neural foramen, suggesting a neurogenic tumor. This posterior mediastinal mass was subsequently biopsy proven to be a paraganglioma.

This condition can arise *de novo*, but more commonly is reactive in a range of clinical scenarios, including recent chemotherapy, burns, autoimmune diseases, chronic inflammation, and myasthenia gravis. In many cases, thymic hyperplasia may be suspected on CT in patients with homogeneous soft tissue interspersed with fat in the expected distribution of the thymus.

When thymic hyperplasia appears more homogeneously solid and mass-like, distinguishing it from neoplasm on CT can be impossible.²⁴ Where there is a high degree of suspicion for neoplasm, such as in treated lymphoma or

myasthenia gravis, MRI can be helpful in characterizing benign thymic tissue. The diagnosis of thymic hyperplasia can be confirmed on MRI with a high degree of confidence if a diffuse drop in tissue signal is observed from in-phase to out-of-phase T1 imaging, indicating the presence of lipid and water in the same voxels (Figure 3).²⁵ However, since not all benign thymic tissue will demonstrate signal loss from in-phase to out-of-phase, diffusion-weighted imaging has been proposed as potentially helpful in distinguishing benign thymic tissue from suspected lymphoma in the anterior mediastinum.²⁶ Since thymic

hyperplasia and many neoplasms are typically FDG-avid on PET/CT, the modality is not considered useful in diagnosing these conditions.²⁷

Proteinaceous cysts

Developmental cysts, such as pericardial or bronchogenic cysts, typically measure simple fluid attenuation on CT, and as low T1 signal and high T2 signal intensity relative to muscle on MRI.²⁸ However, these lesions can sometimes become proteinaceous with CT attenuation values in the range of soft tissue (20-40 HU) and present a diagnostic challenge. Smooth margins, thin walls, chronicity, and lack of internal IV contrast enhancement can suggest benign etiology. MRI can yield a definitive diagnosis of proteinaceous cyst by demonstrating uniform high signal intensity on T1 and T2 imaging.⁹ For patients undergoing FDG-PET/CT, these lesions would be non-FDG avid.

Thymic Cyst

Benign thymic cysts can occur developmentally or, more commonly, are acquired in the context of a variety of chronic inflammatory diseases, including human immunodeficiency virus (HIV),²⁹ and Sjogren syndrome.³⁰ On CT these lesions measure fluid attenuation and are smoothly marginated with thin walls and no internal IV enhancement or solid components. The absence of internal complexity can be confirmed

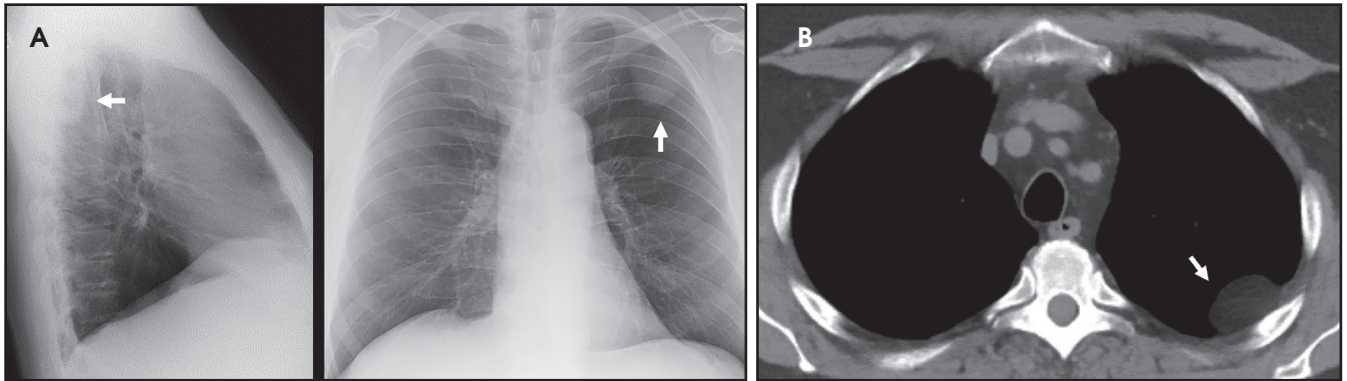


FIGURE 7. Pleural lipoma. (A) Lateral and PA radiographs reveal a peripheral mass (arrows) in the left upper posterior chest of a 65-year-old. The pleural location is suggested by the incomplete boundaries along the lateral aspect of the mass with defined medial borders. (B) On axial unenhanced CT this mass (arrow) is well circumscribed and of homogeneous fat attenuation.

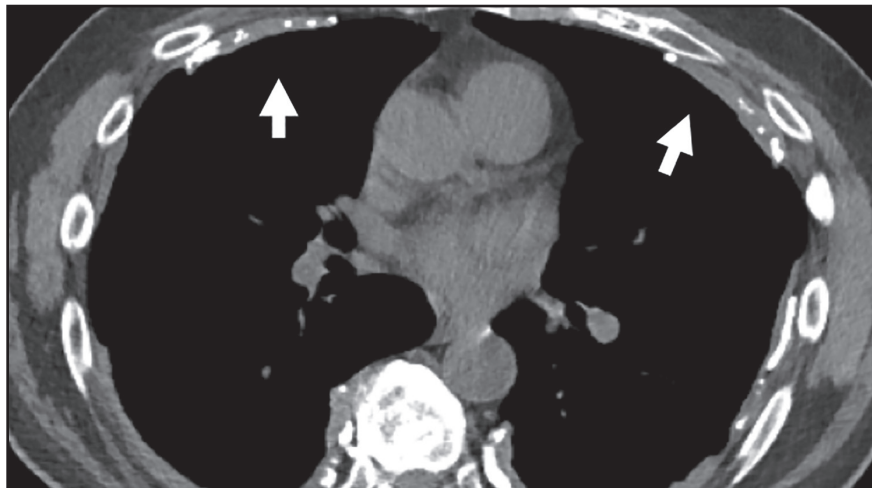


FIGURE 8. Asbestos-related pleural plaques. An axial unenhanced CT of the chest of a 77-year-old with a history of asbestos exposure reveals multiple pleural plaques, some of which have a modest degree of internal calcification.

with MRI, which has an advantage over CT in characterizing the internal complexity of cystic lesions on T2 sequences (Figure 4). The presence of internal solid components or internal enhancement should raise concern for a cystic neoplasm, such as cystic thymoma or thymic carcinoma.^{9,28,31} Benign cysts should also be non-FDG avid on PET/CT.

Mature Cystic Teratomas. A mature cystic teratoma is a benign germ cell tumor usually diagnosed in the anterior mediastinum of asymptomatic young adults, but it occasionally can present symptomatically owing to local mass effect on adjacent structures or, more rarely, to rupture. The classic imaging appearance reflects the presence of all three components of the germ cell layers in varying proportions. On CT these lesions

are well circumscribed and smoothly marginated, containing a mixture of fat, calcium, fluid, and soft-tissue attenuation in variable proportion (Figure 5). The appearance on MRI is typically heterogeneous in signal attenuation on T1 and T2 sequences. Fat-suppression sequences permit detection of macroscopic fat; the presence of fat-fluid level is highly specific for teratomas, though uncommon.^{32,33} Malignant transformation of this tumor is rare; however, a mostly solid lesion, or the presence of an enhancing solid component, can indicate malignancy.³⁴

Neurogenic Tumors. Neurogenic tumors are the most common lesions of the posterior mediastinum, though they are able to grow in a range of anatomical locations, including other mediastinal

compartments and the chest wall. These tumors are divided into autonomic nervous system tumors and nerve sheath tumors, and they can be benign or malignant. Generally, benign nerve sheath tumors demonstrate low attenuation on CT, low signal attenuation on T1 imaging and high signal attenuation on T2 imaging, and enhance homogeneously with IV contrast. These lesions can sometimes be seen insinuating into the ipsilateral neural foramen of the thoracic spine (Figure 6). Ganglioneuroma is a benign, autonomic nervous system tumor found in young children that is usually seen on CT as a well-circumscribed, low-attenuation lesion demonstrating mild enhancement after contrast injection. Fine calcifications are seen in about 20% of patients. On MRI, ganglioneuromas are of homogeneous intensity on all sequences, occasionally demonstrating an internal area of curvilinear low intensity bands.

Schwannomas are benign nerve sheath tumors eccentrically located to the involved nerve.

On CT, schwannomas are seen as soft tissue masses that can contain areas of low attenuation owing to cystic or fatty component, and containing foci of calcium in around 10% of cases; small schwannomas enhance homogeneously. On MRI, these lesions demonstrate intermediate T1 intensity and high T2 intensity relative to muscle, with internal enhancing solid components.

Neurofibromas, also benign nerve sheath tumors, share imaging charac-

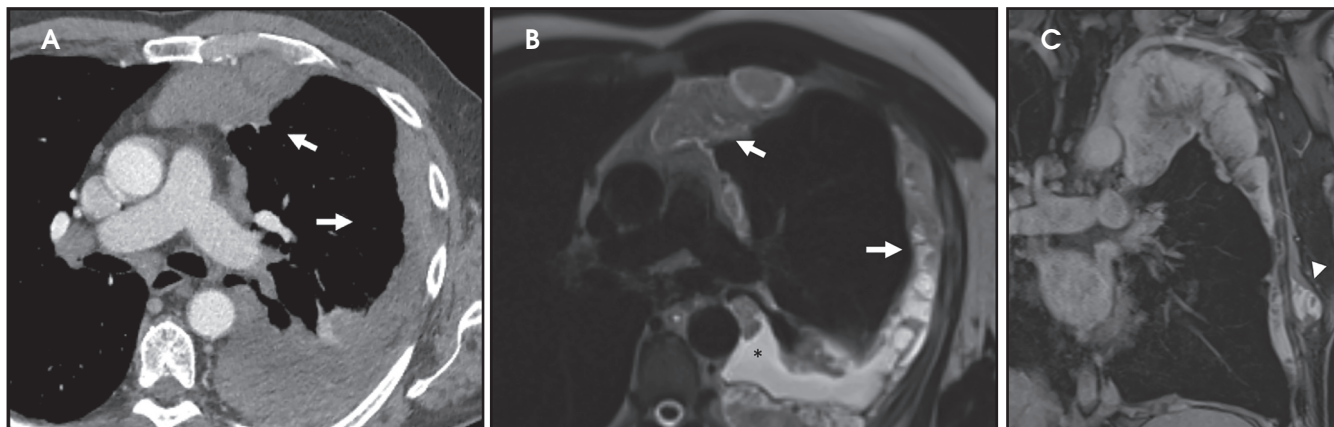


FIGURE 9. Malignant pleural mesothelioma. (A) Axial image of contrast-enhanced (CECT) chest CT of a 63 year-old male demonstrates enhancing circumferential nodular soft tissue in the left pleural space (arrows). Pleural biopsy revealed malignant pleural mesothelioma, epithelioid subtype. (B) Axial T2 MRI reveals the interfaces between pleural fluid (*) and pleural tumor (arrows). (C) Coronal contrast-enhanced MRI reveals enhancing soft tissue invading through the left lateral pleural space into the lateral chest wall soft tissues (arrowhead).

teristics with schwannomas. However, neurofibromas are usually centrally located within the nerve, are more often associated with adjacent bony erosions, and contain internal calcification on CT and slight T2 signal heterogeneity with a brighter, T2 peripheral signal on MRI.

The uncommon malignant counterparts of these lesions will not be discussed but are generally characterized by more heterogeneous imaging appearance on CT and MRI. PET/CT may play a complementary role in distinguishing benign from malignant nerve sheath tumors. A study by Benz et al found FDG-PET/CT to have a sensitivity of 94% and specificity of 91% for malignancy in nerve sheath tumors when the lesions exhibited a standard uptake value (SUV) of 6.1 or greater.³⁵

Pleural Anatomy

The pleura is a membranous structure consisting of two layers, the visceral pleura and the parietal pleura, that create a closed space barrier around each lung. The visceral pleura is closely adherent to the lung parenchyma, with extension into the interlobar fissures, and receives its blood supply from the bronchial arteries. The parietal pleura lines the inner surface of the chest wall, mediastinum, and diaphragm, and receives its blood supply from the intercostal arteries. These two layers are usually closely apposed and lubricated by several mil-

liliters of fluid that assist in holding the layers together with capillary action.^{36,37} In the healthy patient, the full extent of the pleura is not always visible on CT, particularly deep in the posterior sulcus, where no lung apposes the inferior pleural reflection. On average, the boundaries of the pleura occur at 2-3 cm above the first rib superiorly, at the level of 6th or 7th rib anteroinferiorly, and below the 12th rib posteroinferiorly.

Imaging the Pleura Chest Radiography

Pleural thickening, calcification, and fluid can be readily appreciated on chest radiography, although CT is generally more sensitive for assessing the pleura. PA and lateral views are preferred for evaluating the posterior sulcus on the lateral view. A lesion may be suspected to be pleural-based if it is juxtaposed along the pleural surface and exhibits obtuse angles to the pleural surface, with its inner border being sharply margined and its outer border ill defined (*incomplete border sign*, Figure 7).³⁸

Ultrasound

Transthoracic ultrasound is extremely sensitive for the presence of pleural fluid and is useful for characterizing the complexity of pleural fluid. Its low cost and ease of use allows fast, accurate assessment for pleural fluid that can be performed at the bedside

and used to guide thoracentesis. In the emergent setting, US can also be used to rapidly identify pneumothoraces.³⁹

CT

CT is the modality of choice for routine evaluation of the pleura, providing high-resolution imaging of the entire pleura, permitting detection and characterization of subtle pleural abnormalities, including pleural thickening, calcification, and fluid. Pleural findings suspicious for malignancy include: thickness greater than 1 cm, nodularity, and mediastinal pleural thickening.⁴⁰ Intravenous contrast can greatly assist in evaluation of the pleura. In suspected empyema, robust pleural enhancement surrounding a pleural effusion (split pleura sign) is very suggestive of empyema.⁴¹ In pleural malignancy, intravenous contrast provides improved tumor conspicuity and may assist in detecting chest wall, mediastinal, or diaphragmatic invasion.

MRI

With the advantage of superior tissue contrast, MRI can be very useful in defining the extent of pleural disease. For example, MRI is routinely used to assess for diaphragmatic invasion in malignant pleural mesothelioma, which may be underestimated on CT. There is evidence that delayed-phase pleural enhancement may have utility in the MRI evaluation of malignant pleural mesothelioma.⁴² MRI

is also useful for further tissue characterization of pleural lesions, potentially leading to confident diagnosis—for example, in detection of iron-enriched pleural deposits in pleural splenosis. Diffusion-weighted imaging and dynamic contrast enhancement may also be helpful in differentiating benign and malignant pleural tissue.⁴³

FDG-PET/CT

FDG-PET/CT provides information on the metabolic activity of pleural disease and is primarily used as a problem-solving tool for lesions that are indeterminate on CT, as well as to stage malignancy. In malignant pleural mesothelioma, degree of tumor avidity and volume of metabolically active tumor on FDG-PET/CT negativity correlates with survival.⁴⁴⁻⁴⁶ FDG-PET has a very high sensitivity of 95% but only a moderate specificity of 82%⁴⁷ for pleural malignancy. The decreased specificity is attributed to FDG-avid, non-neoplastic inflammatory causes of pleural thickening. Active pleural inflammation, such as that resulting from talc pleurodesis, recent radiation, recent surgery, or a background of pleural plaques, can also confound interpretation of FDG-PET/CT and limit specificity for malignancy.

Multimodality Imaging Applications in the Pleura

Pseudolesions of the Mediastinum:

Functional Pleural Thickening. Apparent subcentimeter focal pleural thickening in the dependent basal aspects of the lung caused by focal alveolar collapse is common, and can be associated with adjacent, ground-glass opacity in the sub-pleural parenchyma. These pseudolesions usually disappear in scans performed in the prone position.⁴⁸

Pleural Pseudotumor. A focal accumulation of pleural fluid in an interlobar fissure, usually the right horizontal fissure, may mimic tumor on a chest radiograph. Most commonly, the pleural position of this collection can be

clarified on the lateral view of the chest radiograph. When in doubt, a chest CT demonstrates typical location and attenuation values that confirm the diagnosis.⁴⁹

Common Challenges for Imaging of the Pleura

Characterization of Pleural Fluid

The complex nature of pleural fluid can be suggested on chest radiography by evidence of fluid loculation. On CT, a detailed distribution of the pleural fluid is possible as well as information on its composition based on attenuation values, which may be in the range of fat (chylothorax), simple fluid (pleural effusion), or hemorrhage (hemothorax). If the presence of fat or blood products is in question, MRI may be helpful, although typically thoracentesis is performed to characterize uncertain pleural fluid collections. A chylothorax may measure fat or fluid attenuation. Pleural effusions typically measure simple fluid attenuation (0-20 HU) and acute hemothorax will demonstrate high attenuation (40-50 HU).

Pleural effusion and nodularity can be an indication of pleural malignancy. In this case pleural effusions are typically accompanied by pleural nodularity, although in some cases the pleural tumor is not detectable on CT. In cases of suspected pleural neoplasm, FDG-PET/CT can be very useful in detecting extent of disease. Combined FDG-PET/CT was shown to have a sensitivity and specificity of 93.5% and 92.6%, respectively.⁵⁰ Dual-energy CT and ultrasound also have demonstrated some utility for characterizing malignant pleural effusions.^{51,52}

Diffuse Pleural Thickening

Pleura thickening can be benign or malignant. Benign thickening is typically smooth, <5 mm in thickness, and spares the mediastinal pleura. It is typically the result of inflammation, most commonly from chronic pleural effusions, empyema, or hemothorax. Benign diffuse pleural thickening can calcify, most often following hemothorax or

empyema, especially empyema with *M. tuberculosis* and, less commonly, following autoimmune pleuritis.⁵³ Both benign and malignant causes of pleural thickening can be FDG-avid on PET/CT; MRI utility is limited in detection of calcification. Pleural thickening that is nodular, circumferential, and involves the medial pleura and >10 mm in thickness is considered suspicious for malignancy.⁵⁴

Pleural Plaques

Discrete focal areas of plaque-like pleural thickening can occur following asbestos exposure, often accompanied by some degree of calcification, and are termed “pleural plaques” (Figure 8). These lesions are typically distributed along the diaphragm and the lower posterolateral ribs. While these changes can usually be appreciated on computed radiography, CT is the modality of choice for characterizing pleural thickening.⁵³ MRI is limited in the detection of calcification. These lesions are often FDG-avid, which can sometimes limit the utility of FDG-PET in characterizing a suspected focus of pleural neoplasm on the background of asbestos-related plaques.

Malignant Pleural Mesothelioma (MPM)

Evidence of focal soft-tissue pleural nodularity or growth at the site of an asbestos-related pleural plaque may indicate development of MPM, a complication that may develop amid 20-30 years' latency following asbestos exposure. MPM can manifest as rind-link pleural thickening, scattered discrete pleural nodules or, less commonly, a single pleural mass. While often visible on CR, CT is the modality of choice, ideally with intravenous contrast enhancement. FDG-PET/CT is usually employed for staging, and MRI is often used to determine the presence or absence of local invasion⁵⁴ (Figure 9).

REFERENCES

1. Fraser RS, Colman NC, Pare PD. *Fraser and Paré's Diagnosis of Diseases of the Chest*. 4th ed. Philadelphia: W.B. Saunders Company; 1999.

2. Felson, B. *Chest roentgenology*. 1st ed. Philadelphia: W.B. Saunders Company; 1973.
3. Fujimoto K, Hara M, Tomiyama N, et al. Proposal for a new mediastinal compartment classification of transverse plane images according to the Japanese Association for Research on the Thymus (JART) General Rules for the Study of Mediastinal Tumors. *Oncol Rep*. 2014;31(2):565-572.
4. Carter BW, Tomiyama N, Bhora FY, et al. A modern definition of mediastinal compartments. *J Thorac Oncol*. 2014;9(9 Suppl 2):S97-101.
5. Carter BW, Benveniste MF, Madan R, et al. ITMIG classification of mediastinal compartments and multidisciplinary approach to mediastinal masses. *Radiographics*. 2017;37(2):413-436.
6. Wernecke K, Vassallo P, Potter R, et al. Mediastinal tumors: sensitivity of detection with sonography compared with CT and radiography. *Radiology*. 1990;175(1):137-143.
7. Tomiyama N, Honda O, Tsubamoto M, et al. Anterior mediastinal tumors: diagnostic accuracy of CT and MRI. *Eur J Radiol*. 2009;69(2):280-288.
8. Miller WT. *Diagnostic Abdominal Imaging*. 1st ed. New York: McGraw-Hill Education; 2012.
9. Madan R, Ratanaprasatporn L, Ratanaprasatporn L, et al. Cystic mediastinal masses and the role of MRI. *Clin Imaging*. 2018; 50:68-77.
10. Inaoka T, Takahashi K, Mineta M, et al. Thymic hyperplasia and thymus gland tumors: differentiation with chemical shift MR imaging. *Radiology*. 2007;243(3):869-876.
11. Shin KE, Yi CA, Kim TS, et al. Diffusion-weighted MRI for distinguishing non-neoplastic cysts from solid masses in the mediastinum: problem-solving in mediastinal masses of indeterminate internal characteristics on CT. *Eur Radiol*. 2014;24(3):677-684.
12. Shim SS, Han J. FDG-PET/CT imaging in assessing mucin-producing non-small cell lung cancer with pathologic correlation. *Ann Nucl Med*. 2010;24(5):357-362.
13. Karam M, Novak L, Cyriac J, et al. Role of fluorine-18 fluoro-deoxyglucose positron emission tomography scan in the evaluation and follow-up of patients with low-grade lymphomas. *Cancer*. 2006;107(1):175-183.
14. Chang JM, Lee HJ, Goo JM, et al. False positive and false negative FDG-PET scans in various thoracic diseases. *Korean J Radiol*. 2006;7(1):57-69.
15. Proli C, De Sousa P, Jordan S, et al. A diagnostic cohort study on the accuracy of 18-fluorodeoxyglucose ((18) FDG) positron emission tomography (PET)-CT for evaluation of malignancy in anterior mediastinal lesions: the DECiMaL study. *BMJ Open*. 2018;8(2):e019471.
16. Cheson BD, Fisher RI, Barrington SF, et al. Recommendations for initial evaluation, staging, and response assessment of Hodgkin and non-Hodgkin lymphoma: the Lugano classification. *J Clin Oncol*. 2014;32(27):3059-3068.
17. Benveniste MF, Moran CA, Mawlawi O, et al. FDG PET-CT aids in the preoperative assessment of patients with newly diagnosed thymic epithelial malignancies. *J Thorac Oncol*. 2013;8(4):502-510.
18. Broderick LS, Brooks GN, Kuhlman JE. Anatomic pitfalls of the heart and pericardium. *Radiographics*. 2005;25(2):441-453.
19. Pinto PS, Sirlin CB, Andrade-Barreto OA, et al. Cisterna chyli at routine abdominal MR imaging: a normal anatomic structure in the retrocrural space. *Radiographics*. 2004;24(3):809-817.
20. Kiyonaga M, Mori H, Matsumoto S, et al. Thoracic duct and cisterna chyli: evaluation with multidetector row CT. *Br J Radiol*. 2012;85(1016):1052-1058.
21. Chen J, Zhang H, Zhu D, et al. Cardiac MRI for detecting left atrial/left atrial appendage thrombus in patients with atrial fibrillation: Meta-analysis and systematic review. *Herz*. 2018.
22. Zou H, Zhang Y, Tong J, et al. Multidetector computed tomography for detecting left atrial/left atrial appendage thrombus: a meta-analysis. *Intern Med J*. 2015;45(10):1044-1053.
23. Molinari F, Bankier AA, Eisenberg RL. Fat-containing lesions in adult thoracic imaging. *AJR Am J Roentgenol*. 2011;197(5):W795-813.
24. Nasserri F, Eftekhari F. Clinical and radiologic review of the normal and abnormal thymus: pearls and pitfalls. *Radiographics*. 2010;30(2):413-428.
25. Priola AM, Priola SM, Ciccone G, et al. Differentiation of rebound and lymphoid thymic hyperplasia from anterior mediastinal tumors with dual-echo chemical-shift MR imaging in adulthood: reliability of the chemical-shift ratio and signal intensity index. *Radiology*. 2015;274(1):238-249.
26. Priola AM, Priola SM, Gned D, et al. Nonsuppressing normal thymus on chemical-shift MR imaging and anterior mediastinal lymphoma: differentiation with diffusion-weighted MR imaging by using the apparent diffusion coefficient. *Eur Radiol*. 2018;28(4):1427-1437.
27. Jerushalmi J, Frenkel A, Bar-Shalom R, et al. Physiologic thymic uptake of 18F-FDG in children and young adults: a PET/CT evaluation of incidence, patterns, and relationship to treatment. *J Nucl Med*. 2009;50(6):849-853.
28. Jeung MY, Gasser B, Gangi A, et al. Imaging of cystic masses of the mediastinum. *Radiographics*. 2002;22 Spec No: S79-93.
29. Kontny HU, Sleasman JW, Kingma DW, et al. Multilocular thymic cysts in children with human immunodeficiency virus infection: clinical and pathologic aspects. *J Pediatr*. 1997;131(2):264-270.
30. Kondo K, Miyoshi T, Sakiyama S, et al. Multilocular thymic cyst associated with Sjogren's syndrome. *Ann Thorac Surg*. 2001;72(4):1367-1369.
31. Ackman JB, Wu CC. MRI of the thymus. *AJR Am J Roentgenol*. 2011;197(1):W15-20.
32. Moeller KH, Rosado-de-Christenson ML, Templeton PA. Mediastinal mature teratoma: imaging features. *AJR Am J Roentgenol*. 1997;169(4):985-990.
33. Patel IJ, Hsiao E, Ahmad AH, et al. AIRP best cases in radiologic-pathologic correlation: mediastinal mature cystic teratoma. *Radiographics*. 2013;33(3):797-801.
34. Gaerte SC, Meyer CA, Winer-Muram HT, et al. Fat-containing lesions of the chest. *Radiographics*. 2002;22 Spec No: S61-78.
35. Benz MR, Czernin J, Dry SM, et al. Quantitative F18-fluorodeoxyglucose positron emission tomography accurately characterizes peripheral nerve sheath tumors as malignant or benign. *Cancer*. 2010;116(2):451-458.
36. Charalampidis C, Youroukou A, Lazaridis G, et al. Pleura space anatomy. *J Thorac Dis*. 2015;7(Suppl 1):S27-32.
37. Finley DJ, Rusch VW. Anatomy of the pleura. *Thorac Surg Clin*. 2011;21(2):157-163, vii.
38. Hsu CC, Henry TS, Chung JH, et al. The incomplete border sign. *J Thorac Imaging*. 2014; 29(4):W48.
39. Marchetti G, Arondi S, Baglivo F, et al. New insights in the use of pleural ultrasonography for diagnosis and treatment of pleural disease. *Clin Respir J*. 2018;12(6):1993-2005.
40. Leung AN, Muller NL, Miller RR. CT in differential diagnosis of diffuse pleural disease. *AJR Am J Roentgenol*. 1990;154(3):487-492.
41. Kraus GJ. The split pleura sign. *Radiology*. 2007;243(1):297-298.
42. Patel AM, Berger I, Wileyto EP, et al. The value of delayed phase enhanced imaging in malignant pleural mesothelioma. *J Thorac Dis*. 2017;9(8):2344-2349.
43. Coolen J, De Keyzer F, Nafteux P, et al. Malignant pleural disease: diagnosis by using diffusion-weighted and dynamic contrast-enhanced MR imaging—initial experience. *Radiology*. 2012; 263(3):884-892.
44. Kitajima K, Doi H, Kuribayashi K, et al. Prognostic value of pretreatment volume-based quantitative (18)F-FDG PET/CT parameters in patients with malignant pleural mesothelioma. *Eur J Radiol*. 2017; 86:176-183.
45. Nowak AK, Francis RJ, Phillips MJ, et al. A novel prognostic model for malignant mesothelioma incorporating quantitative FDG-PET imaging with clinical parameters. *Clin Cancer Res*. 2010;16(8):2409-2417.
46. Francis RJ, Byrne MJ, van der Schaaf AA, et al. Early prediction of response to chemotherapy and survival in malignant pleural mesothelioma using a novel semiautomated 3-dimensional volume-based analysis of serial 18F-FDG PET scans. *J Nucl Med*. 2007;48(9):1449-1458.
47. Treglia G, Sadeghi R, Annunziata S, et al. Diagnostic accuracy of 18F-FDG-PET and PET/CT in the differential diagnosis between malignant and benign pleural lesions: a systematic review and meta-analysis. *Acad Radiol*. 2014;21(1):11-20.
48. Claude-Desroches M, Bierry G, Touitou-Gotenberg D, et al. Focal dependent pleural thickening at MDCT: pleural lesion or functional abnormality? *Diagn Interv Imaging*. 2012;93(5):360-364.
49. de Paula MC, Escuissato DL, Belem LC, et al. Focal pleural tumorlike conditions: nodules and masses beyond mesotheliomas and metastasis. *Respir Med*. 2015;109(10):1235-1243.
50. Sun Y, Yu H, Ma J, et al. The role of 18F-FDG PET/CT integrated imaging in distinguishing malignant from benign pleural effusion. *PLoS One*. 2016;11(8):e0161764.
51. Zhang X, Duan H, Yu Y, et al. Differential diagnosis between benign and malignant pleural effusion with dual-energy spectral CT. *PLoS One*. 2018;13(4):e0193714.
52. Bugalho A, Ferreira D, Dias SS, et al. The diagnostic value of transthoracic ultrasonographic features in predicting malignancy in undiagnosed pleural effusions: a prospective observational study. *Respiration*. 2014;87(4):270-278.
53. Walker CM, Takasugi JE, Chung JH, et al. Tumorlike conditions of the pleura. *Radiographics*. 2012;32(4):971-985.
54. Nickell LT, Lichtenberger JP, Khorashadi L, et al. Multimodality imaging for characterization, classification, and staging of malignant pleural mesothelioma. *Radiographics*. 2014;34(6):1692-1706.